of MET suggests that in addition to up-regulated TFE3 fusion protein expression, as shown by preclinical assays [12], activation of RET may also occasionally occur after activation of MET by the HGF ligand. Currently, no data are available on the activity of sunitinib on MET. However, SU5416, another RTK inhibitor, that is chemically related to sunitinib and has similar functional groups, inhibits the activation of HGF/MET in hepatocellular carcinoma. This suggests that sunitinib might be involved in the HGF/MET down-signaling switch off [13].

This case study illustrates the efficacy of sunitinib in metastatic RCC associated with Xp11.2 translocation. However, further studies are required to confirm the clinical benefits of RTK inhibitors in patients with this type of RCC.

Conflict of interest No author has any conflict of interest.

References

1. Argani P, Antonescu CR, Illei PB et al (2001) Primary renal neoplasms with the *ASPL-TFE3* gene fusion of alveolar soft part sarcoma. Am J Pathol 159:179–192
2. Motzer RJ, Hutson TE, Tomczak P et al (2009) Overall survival and updated results for sunitinib compared with interferon alfa in patients with metastatic renal cell carcinoma. J Clin Oncol 27:3584–3590
3. Winarti NW, Argani P, De Marzo AM et al (2008) Pediatric renal cell carcinoma associated with Xp11.2 translocation/*TFE3* gene fusion. Int J Surg Pathol 16:66–72
4. Choueiri TK, Mosquera JM, Hirsch MS (2009) A case of adult metastatic Xp11 translocation renal cell carcinoma treated successfully with sunitinib. Clin Genitourin Cancer 7:93–94
5. Zhong M, De Angelo P, Osborne L et al (2010) Dual-color, break-apart FISH assay on paraffin-embedded tissues as an adjunct to diagnosis of Xp11 translocation renal cell carcinoma and alveolar soft part sarcoma. Am J Surg Pathol 34:757–766
6. Tsuda M, Davis IJ, Argani P et al (2007) TEF3 fusions activate MET signaling by transcriptional up-regulation, defining another class of tumors as candidates for therapeutic MET inhibition. Cancer Res 67:919–929
7. Malouf GG, Camparo P, Oudard S et al (2010) Targeted agents in metastatic Xp11 translocation/TFE3 gene fusion renal cell carcinoma (RCC): a report from the Juvenile RCC Network. Ann Oncol 21:1834–1838
8. Mendel DB, Laird AD, Xin X et al (2003) In vivo antitumor activity of SU11248, a novel tyrosine kinase inhibitor targeting vascular endothelial growth factor and platelet-derived growth factor receptors: determination of a pharmacokinetic/pharmacodynamic relationship. Clin Cancer Res 9:327–337
9. O'Farrell AM, Abrams TJ, Yuen HA et al (2003) SU11248 is a novel FLT3 tyrosine kinase inhibitor with potent activity in vitro and in vivo. Blood 101:3597–3605
10. Chow LQM, Eckhardt SG (2007) Sunitinib: from rational design to clinical efficacy. J Clin Oncol 25:884–896
11. Stacchiotti S, Tamborini E, Marrari A et al (2009) Response to sunitinib malate in advanced alveolar soft part sarcoma. Clin Cancer Res 15:1096–1104
12. Ivan M, Bond JA, Prat M et al (1997) Activated ras and ret oncogenes induce over-expression of c-met (hepatocyte growth factor receptor) in human thyroid epithelial cells. Oncogene 14:2417–2423
13. Wang SY, Chen B, Zhan YQ et al (2004) SU5416 is a potent inhibitor of hepatocyte growth factor receptor (c-Met) and blocks HGF-induced invasiveness of human HepG2 hepatoma cells. J Hepatol 41:267–273

Citation: Blood Cancer Journal (2011) 1, e15; doi:10.1038/bcj.2011.11

www.nature.com/bcj

ORIGINAL ARTICLE

The identification of irreversible rituximab-resistant lymphoma caused by *CD20* gene mutations

Y Mishima[1,2], Y Terui[1], K Takeuchi[3], Y Matsumoto-Mishima[1], S Matsusaka[1], R Utsubo-Kuniyoshi[1,2] and K Hatake[1]

[1]Department of Clinical Chemotherapy, Cancer Chemotherapy Center, Japanese Foundation for Cancer Research, Tokyo, Japan; [2]Olympas Bio-Imaging Lab, Cancer Chemotherapy Center, Japanese Foundation for Cancer Research, Tokyo, Japan and [3]Division of Pathology, Cancer Institute, Japanese Foundation for Cancer Research, Tokyo, Japan

C-terminal mutations of CD20 constitute part of the mechanisms that resist rituximab therapy. Most CD20 having a C-terminal mutation was not recognized by L26 antibody. As the exact epitope of L26 has not been determined, expression and localization of mutated CD20 have not been completely elucidated. In this study, we revealed that the binding site of L26 monoclonal antibody is located in the C-terminal cytoplasmic region of CD20 molecule, which was often lost in mutated CD20 molecules. This indicates that it is difficult to distinguish the mutation of CD20 from under expression of the CD20 protein. To detect comprehensive CD20 molecules including the resistant mutants, we developed a novel monoclonal antibody that recognizes the N-terminal cytoplasm region of CD20 molecule. We screened L26-negative cases with our antibody and found several mutations. A rituximab-binding analysis using the cryopreserved specimen that mutation was identified in CD20 molecules indicated that the C-terminal region of CD20 undertakes a critical role in presentation of the large loop in which the rituximab-binding site locates. Thus, combination of antibodies of two kinds of epitope permits the identification of C-terminal CD20 mutations associated with irreversible resistance to rituximab and may help the decision of the treatment strategy.
Blood Cancer Journal (2011) **1,** e15; doi:10.1038/bcj.2011.11; published online 8 April 2011
Keywords: B-cell lymphomas; mutations; antibody therapy; CD20; rituximab

Introduction

Previously, we reported that gene mutations of *CD20* were somehow involved in resistance to rituximab therapy, and we proposed that C-terminal deletion mutations of CD20 might be related to relapse/resistance after rituximab therapy.[1] Many of these C-terminal truncated CD20 molecules were not recognized by the L26 monoclonal antibody used routinely in most clinical laboratories. Therefore, expression of CD20 seemed to have been completely lost for these lymphomas. However, an immunohistochemical study using a polyclonal antibody showed that some kind of C-terminal truncated CD20 was present in cytoplasm, so it was possible that the epitope of L26 was lost by gene mutations.[1] L26 recognizes the cytoplasmic region of CD20 molecules, but no more detailed information about its epitope had been reported.[2,3] In this study, we determine a recognition site of L26 by using a series of deletion mutants of CD20 molecules. In addition, to detect every one of the mutated CD20 molecules, we developed new antibodies that recognize the N-terminal region of CD20 molecules. We used these antibodies to identify cells that have CD20 molecules with abnormalities in the C-terminal cytoplasmic region. We characterized these mutated CD20 molecules using living primary lymphoma cells.

Correspondence: Dr K Hatake, Department of Clinical Oncology and Hematology, Cancer Institute Hospital, Japanese Foundation for Cancer Research, 3-8-31, Ariake Koto-ku, Tokyo 135-8550, Japan.
E-mail: khatake@jfcr.or.jp
Received 28 October 2010; revised 7 January 2011; accepted 1 February 2011

Materials and methods

Cells, viruses and DNA constructs

The coding region of the *CD20* gene was amplified by reverse transcription PCR (RT-PCR) from RNA extracted from a Burkitt's lymphoma cell line, Raji, and was cloned into a pDON-AI retroviral vector (Takara, Ohtsu, Japan). A series of deletion mutants of CD20 in the C-terminal cytoplasmic region was constructed by inserting stop codons after nucleotides encoding E281, E263, E245, V228 and G210. Retroviruses carrying wild type and deletion mutants of *CD20*, together with mock construct, were produced with the transient retrovirus packaging cell line G3T-hi (Takara) according to the manufacturer's protocol. Packaged retrovirus vectors were then used to infect a myeloma cell line, KMS12PE,[4] with subsequent selection using 500 μg/ml G418.

For the transfection of mutant *CD20* gene, whole coding region of *CD20* complementary DNA (cDNA) prepared by RT-PCR of total RNA isolated from the patient cells was cloned into first cassette of a bicistronic retrovirus vector carrying a green fluorescent protein (Takara). Bicistronic expression of ZsGreen is facilitated by internal ribosomal entry site only when *CD20* mutant gene was translated, enabling the efficient selection of transformed cells.

Generation of monoclonal antibody secreting hybridomas

A synthetic peptide corresponding to residues 23–36 of human CD20 with one additional cysteine at the N-terminus (CMQSGPKPLFRRMSS) was synthesized. The peptide was coupled with keyhole limpet hemocyanin. BALB/c mice were primed with a subcutaneous injection of the keyhole limpet hemocyanin-conjugated synthetic peptide emulsified in Freund's complete adjuvant. Mice were boosted four times at two-week intervals with the same antigen. Mice that developed antibodies as measured by enzyme-linked immunosorbent assay with the immunizing peptide were boosted intravenously with the same peptide 4 days before splenocytes were harvested and fused to mouse myeloma cells. Hybridization and cloning were performed according to standard procedures.[5]

CD20 gene sequencing

Pleural effusion mononuclear cells were obtained by density gradient centrifugation using Ficoll-Hypaque 1.077 (Sigma,

St Louis, MO, USA). The isolated mononuclear cells then underwent negative immunomagnetic selection using a B Cell Isolation Kit II (Miltenyi Biotec, Bergisch Gladbach, Germany) for purifying B-linage cells. Total RNA was prepared using TRIzol reagent according to the instructions of the manufacturer (Invitrogen, Carlsbad, CA, USA) and 1 μg was subjected to reverse transcription under MMLV reverse transcriptase (Takara). To prepare cDNA-containing whole coding region of *CD20*, PCR amplification was performed from 2 μl of cDNA using primers outside of the start and the stop codon: hCD20-5′-FW (5′-GCAGCTAGCATCCAAATCAG-3′) and hCD20-3′-RV (5′-TGGTGCGTATGTGCAGAGTA-3′). To determine the sequence of the *CD20*, we performed cycle sequencing on a 3130 DNA analyzer (Applied Biosystems, Foster City, CA, USA), directly from PCR-purified products, in both directions using a BigDye Terminator Cycle Sequencing Kit v3.1 (Applied Biosystems).

Immunocytochemistry

Cells were stained by rituximab and L26 antibody (DAKO, Carpentaria, CA, USA) sequentially. Briefly, the cells were labeled by incubating in 10 μg/ml of rituximab conjugated with Alexa Fluor 647 (Invitrogen) according to previously described procedure[6] and washed twice with phosphate-buffered saline. Rituximab-labeled cells were swelled by treatment with 75 mM KCl and then were made to adhere onto collagen I-coated cover glass by brief centrifugation. After fixing and permeabilization, the specimens were exposed to L26 antibody. Subsequently, the specimens were washed and were incubated in Alexa488-conjugated goat anti-mouse IgG. Nuclear staining was performed using 5 μg/ml of 4′-6-diamidino-2-phenylindole. The preparations were screened for fluorescence with a confocal microscope (FV1000, OLYMPUS, Tokyo, Japan) using excitation wavelengths of 405, 488 and 633 nm to detect emission by nuclear staining (4′-6-diamidino-2-phenylindole), rituximab or L26 staining, respectively.

Immunohistochemistry

The tissues had been routinely fixed in 10% neutral formalin and embedded in paraffin. L26 antibody and monoclonal antibodies raised against the N-terminal cytoplasmic region of CD20 were used. The sections were deparaffinized and rehydrated in graded alcohol. For heat-induced epitope retrieval, the sections were subjected to Target Retrieval Solution, pH 9 (DAKO) at 97 °C for 40 min. The sections then were brought to an automated stainer (DAKO) by following the vendor's protocol. EnVision Plus (DAKO) and peroxidase detection methods were used.

Rituximab-binding analysis

Rituximab-binding analysis was performed according to our previously developed imaging-based procedure, with some modifications.[6] Briefly, approximately ten thousands cells of purified living lymphoma cells using a Dead cell removal kit (Miltenyi Biotec) were incubated with 10 μg/ml of anti-CD19 mAb labeled with Alexa Fluor 488 (Invitrogen) and rituximab labeled with Alexa Fluor 647 (Invitrogen) for 30 min at 4 °C. The cells were washed with phosphate-buffered saline two times and were then suspended in 4 μl of RPMI1640 medium supplemented with 10% fetal bovine serum and 5 μg/ml of Hoechist 33 342. The cell suspension was pipetted into a well made of silicon, 2.5 mm in diameter and 2 mm in depth, on a piece of cover glass. Images were collected by means of an OLYMPUS PlanApo ×60 oil objective in an OLYMPUS FV-1000 confocal microscope (OLYMPUS). The fluorophore was excited by laser at 405, 488 or 633 nm. The cells were optically sectioned along the *z*-axis, and the images were collected at 640 × 640 pixel resolution in a sequential mode to minimize the crossover between channels. The step size in the *z*-axis was 0.5 μm. For three-dimensional reconstruction, two-dimensional confocal stacks were saved in an Olympus.oib format and three-dimensional images were generated using Fluoview software (OLYMPUS).

Cell sorting and genetic analysis

The cryopreserved B-linage cells of the pleural effusion at relapse were further sorted into two fractions of the cells with high affinity to rituximab (R-high) and those of low (R-low) by using flow cytometry (FACSvantage, Becton Dickinson, Franklin Lakes, NJ, USA). The cells were labeled with rituximab conjugated with AlexaFluor488 (Invitrogen) and anti-CD19-PE (Becton Dickinson), then resuspended in phosphate-buffered saline containing 2 μg/ml of 7-AAD (Sigma) to exclude dead cells. The sorting gate used for 'R-high' was rituximab^{high}/CD19^{+}/7-AAD^{-}, and for 'R-low' was rituximab^{low}/CD19^{+}/7-AAD^{-}. The sorted cells were immediately used for extraction of both genomic DNA and total RNA using QIAamp DNA micro kit and RNeasy micro kit, respectively, (QIAGEN, Hilden, Germany). For amplifying the DNA-containing exon 8 of *CD20* from genomic DNA, PCR was carried out using the forward primer (5′-TTCTGTTTTZGAACATAGTTCTCCCTGTCCA-3′) and the reverse primer (5′-CAGAAAACAGAAATCACTTAAGGAGAG-3′). RT-PCR to amplify the *CD20* cDNA were performed according to the method described above. The PCR and RT-PCR products were used to determine the *CD20* gene sequence by direct sequencing method. In addition, 1 μl of RT-PCR products were cloned into a TA-cloning vector (pCR2.1, Invitrogen) and *CD20* DNA sequences of 16 clones of each RT-PCR product were determined for estimating the ratio of different sequences.

Results

To confirm the epitope of L26, we made a series of constructs of the CD20 molecules with deletion mutations in the C-terminal cytoplasmic domain and introduced them into retrovirus vectors (Figure 1a). KMS12PE cells, in which expression of CD20 is not detected immunohistologically, were then transformed, and we established six kinds of sub-lines with the various C-terminal deletion mutations of CD20. A semi-quantitative RT-PCR analysis using a primer set designed to amplify the *CD20* N-terminal region indicated that no major difference was found in *CD20* messenger RNA (mRNA) expression of the six cell lines (Figure 1b). We carried out immunocytochemical analysis using L26 and fluorescence-labeled rituximab against these six *CD20*-expressing transfectants, along with a mock transfectant and Raji cells as negative and positive controls, respectively. The cells stained by L26 antibody were only those expressing wild type (amino acid 1–297) and DM1 mutant (amino acid 1–281). On the other hand, rituximab could bind to shorter CD20 molecules, such as DM2, DM3 or DM4, as well as to the CD20 molecules recognized by L26 (Figure 1c). These results indicate that L26 antibody recognizes the C-terminal cytoplasm region of CD20 molecules and that its epitope is present in the amino-acid sequence of 264–281. The data suggest that immunohistochemistry using L26 antibody will exhibit a false negative if a deletion or a frame shift occurs upstream of this epitope. In addition, the shortest deletion mutant DM5 that lacked the C-terminal cytoplasmic region was detected by

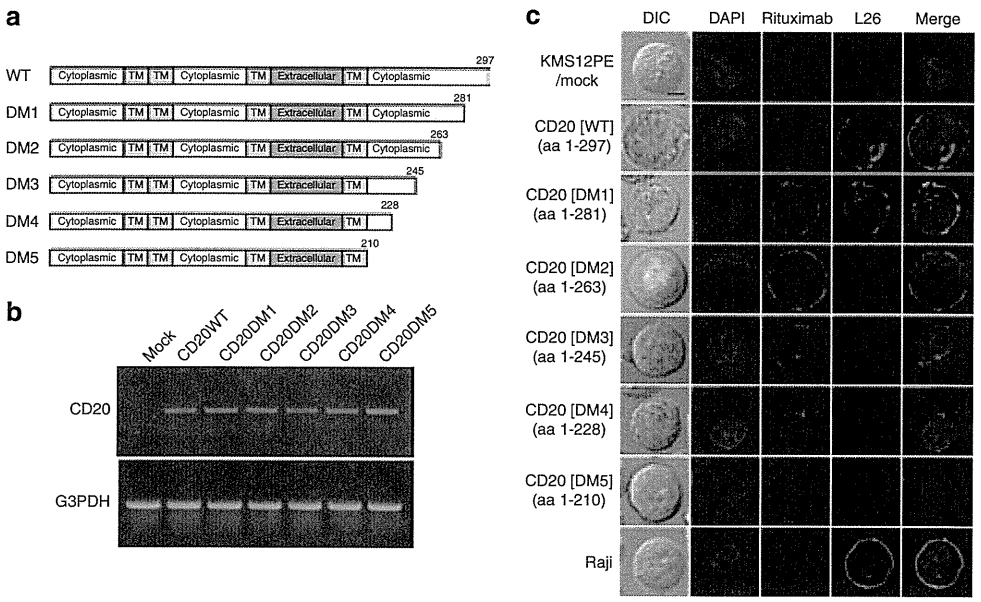

Figure 1 Search for epitopic site of L26 antibody and analysis of the extracellular exposure of CD20 molecules having C-terminal deletion mutation. (**a**) To explore the binding site of the L26 antibody, we constructed various lengths of the CD20 deletion mutant at their C-terminal cytoplasmic domains. TM: transmembrane domain. (**b**) KMS12PE cells retrovirally transduced with C-terminal truncated CD20 showed approximately similar levels of mRNA expression. (**c**) Immunocytochemical studies suggested that L26 recognizes amino-acid sequence between 264 and 281. An objective lens of × 60 was used with a × 10 digital zoom, bar: 5 μm. DAPI, 4′-6-diamidino-2-phenylindole; DIC, differential interference contrast; G3PDH, glyceraldehyde-3-phosphate dehydrogenase; WT, wild type.

neither L26 antibody nor rituximab. Possible reasons might include the low membrane localization of DM5 mutant and/or low stability of the post-translational product. To clarify this, we carried out western blot analysis using total cell lysate of the series of deletion mutants that were tagged by FLAG peptide at the N-terminal region of CD20 constructs. We found that the cellular protein level of the DM5 deletion mutant of CD20 was remarkably lower than that of others, suggesting that low post-translational stability may be the reason for the low antigenicity of DM5 mutant (data not shown).

To detect CD20 in the clinical specimens that acquired rituximab resistance mutations, we developed novel anti-CD20 antibodies and screened them in paraffin sections. We isolated an antibody specific for the CD20 N-terminus and named it CD20N. Using this antibody, we carried out immunohistochemistry conducted on the CD20-negative cases by L26 antibody-based analysis and found several cases with mutations in the C-terminal cytoplasm region. Among them, a cell specimen, a part of which had been cryopreserved as living cells, was included. This was pleural effusion from a patient with relapsed diffuse large cell B-cell lymphoma after complete remission following rituximab containing chemotherapy (rituximab, cyclophosphamide, adriamycin, vincristine and prednisone). This patient did not respond to further treatment with salvage therapies containing rituximab. The results of immunochemical analysis of the fibrin clot of the pleural effusion at relapse, as well as the biopsy of lymph nodes at the first examination, are shown in Figure 2. The lymph node biopsy before rituximab treatment was stained in the same way by both L26 and CD20N antibodies. However, L26 antibody did not stain at the population having mutated CD20 in the pleural effusion. On the other hand, the CD20N antibody stained almost all of the B-cell population. It should be noted that most of the cells were stained at the region of plasma membrane by CD20N antibody.

As a result of DNA sequencing of purified B cells, we found one nucleotide deletion mutation, which caused a frame shift after the amino-acid residue 251, in half of the DNA (Figure 3a). We conducted a binding analysis of rituximab using the viable cells of B-lineage purified from cryopreserved mononuclear cells. Most of these cells were CD19 positive. However, these cells consisted of two kinds of cell populations that were quite different in their affinity for rituximab (Figure 3b). Furthermore, flow cytometry analysis revealed that the fluorescent intensity of fluoro-labeled monoclonal antibody of CD20 decreased to less than one-tenth in about half of the B-cell population (Figure 3c). These results indicate that the C-terminal mutation of the *CD20* gene in this case caused abnormality of extracellular-antigen presentation, even though the protein expression and the cell membrane localization seemed to be normal.

To reveal the genetic mechanisms of the reduced antigenicity to rituximab, we conducted gene-sequencing analysis about both population of cells that differ in affinity to rituximab. The cryopreserved B lymphocytes of the pleural effusion at relapse were sorted into two fractions of cells of high affinity to rituximab (R-high) and those of low (R-low) by using flow cytometry (Figure 4a). Then genomic DNA and total RNA from each fraction were extracted. The results of DNA sequencing of exon 8 of *CD20* in which the mutation was found demonstrated that, surprisingly, both cell populations had both normal and the monobasic deletion mutant *CD20* genes. To determine the proportion of the genes, the PCR-amplified DNA fragments were inserted into a TA-cloning vector and 16 clones from both 'R-high' and 'R-low' fractions were determined the sequence of *CD20*. As a result, the ratio of mutant DNA accounted for approximately half of genomic DNA of both 'R-high' (7 out of 16) and 'R-low' (9 out of 16). On the other hand, the results of sequence analysis about the cDNA revealed that the ratio of mutant mRNA in 'R-low' was remarkably increased (14 out of 16), whereas that of 'R-high' was as the same of the results of genomic DNA (8 out of 16; Figure 4b). We also carried out a sequence analysis about genomic DNA from a slice of paraffin -embedded tissue of lymph node at the first diagnosis of this patient, and found that approximately half of the genomic DNA

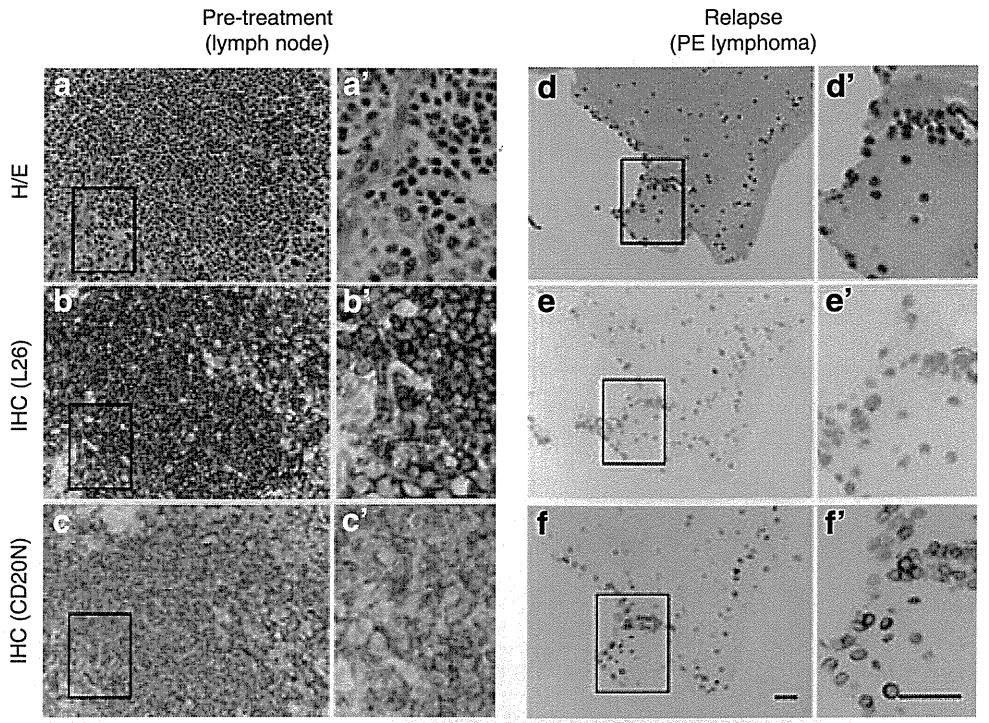

Figure 2 Immunohistochemistry (IHC) was performed on a biopsied specimen of a lymph node at the first examination (**a**, **b** and **c**) and on a fibrin clot from the B-cell population from pleural effusion at the relapse phase (**d**, **e** and **f**). Both L26 and CD20N antibodies uniformly stained the lymphoma cells in the lymph node biopsy specimen (**b** and **c**, respectively). However, L26 did not recognize about half of the B cells derived from pleural effusion (**e**), whereas CD20N stained almost all the cells (**f**). (**a** and **d**) indicates hematoxylin and eosin (H/E) stain. High-magnification images of the region boxed in (**a**–**f**) were shown in (**a'**–**f'**), respectively. An objective lens of × 60 was used, bar: 50 μm. PE lymphoma, lymphoma cell in pleural effusion.

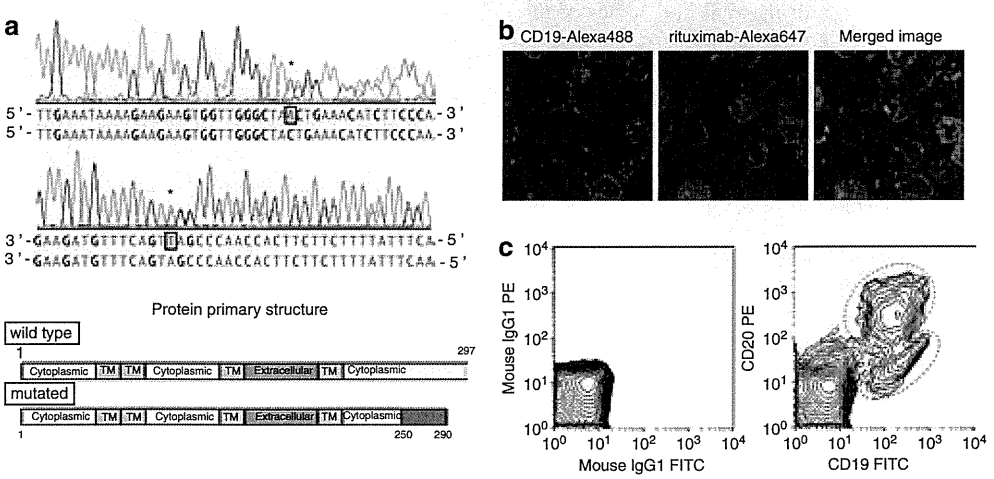

Figure 3 The analysis of primary lymphoma cells derived from pleural effusion of a patient with rituximab-refractory, diffuse large-cell lymphoma. (**a**) A direct sequence analysis of the CD20-coding region revealed that an adenine residue (+478) was deleted in about half of the cDNA. This gene mutation caused a frame shift after the amino-acid sequence of 250 and early denomination. The blue column in the protein schematic charts expresses an abnormal primary structure. *Single nucleotide deletion occurred at this position in approximately half of cDNA. (**b**) Rituximab-binding analysis based on three-dimensional imaging. Magnetically sorted living B-lineage cells were labeled with CD19 (green pseudo-color) and rituximab (red pseudo-color). Although the intensity varied, the CD19 antigen was expressed in most of the cells. Meanwhile, rituximab bound markedly to approximately half of the cells, but the binding to the rest of cells could not be detected. The blue pseudo-color indicates fluorescence of Hoechist22242 nuclear dye. Results shown here are representative of the 19 microscopic fields. (**c**) Flow cytometric analysis of mononuclear cells from the pleural effusion of this patient suggested that there were two populations of different CD20-expressing levels among CD19 positive cells. The mean fluorescence intensities (MFIs) of the higher (blue) and lower (red) CD20-expressing populations were calculated as 486.8 and 30.5, respectively. FITC, fluorescein isothiocyanate.

included the mutant *CD20* gene same as the cells at relapse (8 out of 16; Figure 4c). These results indicated that this patient had already carried the mutation in *CD20* gene, as onset of primary lymphoma, and that a transcriptional imbalance of wild-type *CD20* and mutated *CD20* have occurred by undetermined mechanisms in some cell populations.

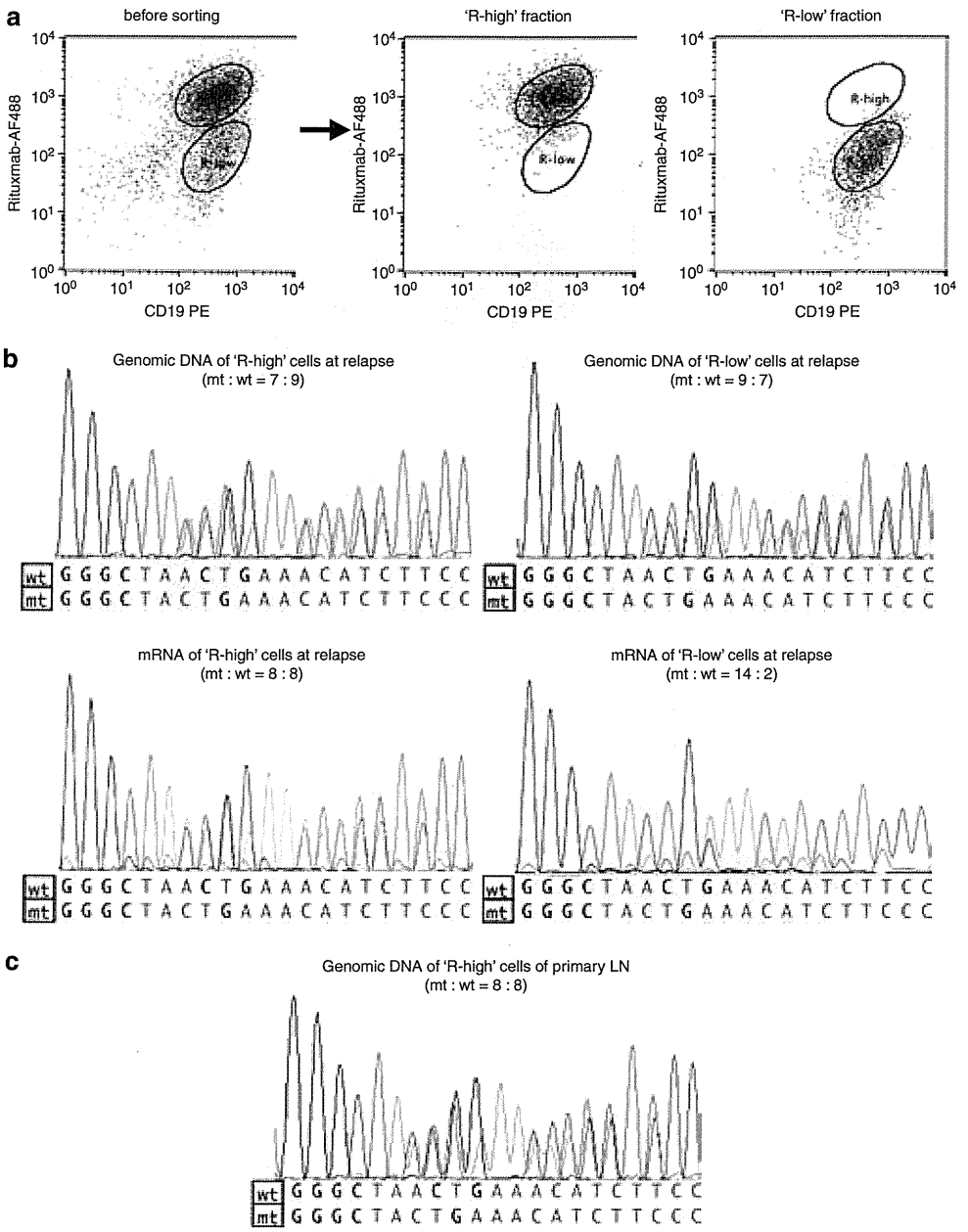

Figure 4 The genetic analysis of patient's lymphoma cells. The cryopreserved B linage cells of the pleural effusion at relapse were further sorted into two fractions of cells with high affinity to rituximab (R-high) and those of low (R-low) by using flow cytometry. (**a**) Dot blot of the cells before and after sorting. (**b**) The results of CD20 sequence analysis of genomic DNA and cDNA of 'R-high' and 'R-low'. The diagrams of direct sequencing of CD20 exon 8 region are shown. The ratio of mutant and wild-type *CD20* genes were determined by the sequencing of 16 clones of RT-PCR products. (**c**) The results of genomic DNA sequence of primary lymphoma.

As CD20 is thought to be present as a tetramer in cells,[7] mutated CD20 may affect also wild-type peptide in the same cell. To verify this possibility, we introduced the *CD20* gene carrying the same mutation as this patient to $CD20^-$ cell line, KMS12PE and $CD20^+$ Daudi using a retrovirus vector, then selected the cells expressing the exogeneous *CD20* by a green fluorescent protein reporter promoted by an internal ribosome entry site (Figure 5a). As the result of evaluating the binding affinity to rituximab by flow cytometry, the exogeneous mutated CD20 exhibited remarkably attenuated antigenicity to rituximab as compared with the wild-type CD20 (Figure 5b). Next, we transformed Daudi cells with the mutant *CD20* to examine the effect on expression of wild-type CD20 molecules. In consideration of turnover of intrinsic CD20, we evaluated binding of rituximab to the transfectants 7 days after virus infection. As shown in Figure 5c, the expression of this mutated CD20 was found to have hardly affected the affinity for rituximab. These results suggested that at least the mutation found in this patient did not exert a dominant negative effect against normal CD20 molecules.

Discussion

Previously, we reported that mutations in the *CD20* gene were found with some frequency in patients treated with rituximab.

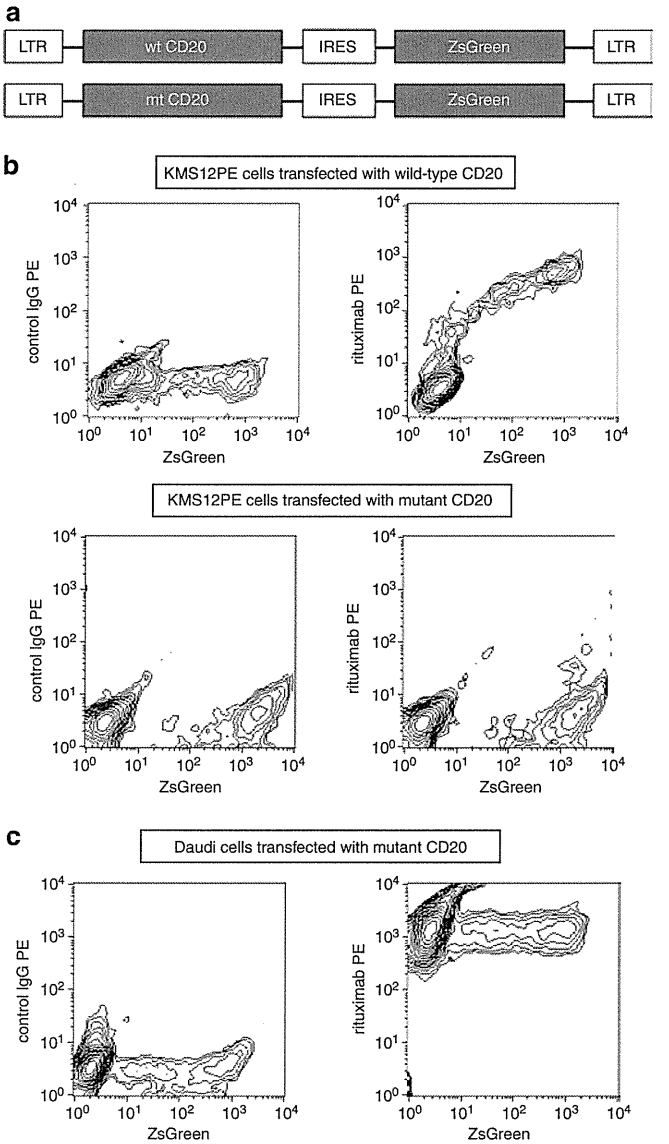

Figure 5 The effect of mutant *CD20* on wild-type *CD20* with respect to rituximab binding. (**a**) The schematic diagram of retrovirus vectors used for transduction of wild-type and mutant *CD20*. (**b**) The transfectants were labeled with PE-conjugated. rituximab and analyzed by flow cytometry at seven days after viral infection. The contour plots of KMS12PE cells transfected with wild-type (upper panel) or mutated *CD20* (lower panel) are shown. (**c**) Daudi cells were transfected with mutated *CD20* and analyzed the rituximab-binding. The mutant *CD20* introduced exogenously hardly affected the binding of rituximab to Daudi cells. IRES, internal ribosome entry site; LTR, long terminal repeat; wt, wild type; mt, mutant.

These cases often have a diagnosis of CD20 negative by immunostaining, based on the commonly used L26 antibody, and are difficult to distinguish from the cases in which protein expression of CD20 is extremely low. So the mutation in the *CD20* gene has been less noticed with regard to resistance to rituximab. In the present study, we roughly identified the epitope of L26, and it became clear that all of the C-terminal-mutated CD20 that we had found earlier lost the epitope for L26, because the epitope was located near the C-terminal of CD20 molecule. To detect CD20 with these mutations comprehensively, we developed monoclonal antibodies that recognize a part of the amino-acid sequence of the N-terminal cytoplasmic region of CD20. One of these antibodies, CD20N, recognized CD20 proteins, including those having a mutation in the paraffin-embedded, formalin-fixed specimen. In this study, we showed that it could be applied to the primary screening of the lymphoma cells that express mutated CD20 by selecting L26-negative and CD20N-positive cells.

To date, there are not many reports that the mutation of the *CD20* gene contributes to resistance to rituximab.[1,8] A part of the reason for this may be that L26 cannot detect most of mutated CD20. In addition, Johnson *et al.*[8] carried out a sequencing screening of exon 5 of the *CD20* gene encompassing the epitope of rituximab. They detected *CD20* mutations involving the rituximab epitope in only 1/264 (0.4%) and 1/15 (6%) of the biopsies taken at diagnosis and relapse, respectively. Similarly, in our previous screening, no mutation was found in the region of exon 5, whereas four cases with mutation (out of 50) were found in the C-terminal cytoplasm region of CD20.[1] In the *CD20* gene, a genetic mutation could be more likely to occur in the C-terminal region compared with around the region of rituximab epitope by uncertain mechanism(s).

By using live cryopreserved cells, derived from a newly identified case with the mutation in the *CD20* gene, we successfully analyzed in detail the phenotype of lymphoma cells having mutated CD20. In this case, a frame shift mutation occurred because of one base nucleotide deletion, resulting in the translation of peptide of another reading frame of 41 amino acids after the amino acid position 250 with a slight early termination. Immunohistochemical analysis using CD20N antibody revealed that the CD20 molecules with C-terminal mutations were indeed expressed in the lymphoma cells, and located at the cell membrane. However, the living cell binding evaluation showed that rituximab could scarcely bind to these cells. These results suggest that the C-terminal region of CD20 undertakes a critical role in presentation of the large loop in which the rituximab-binding site locates.

As a result of genetic analysis for lymphoma cells, it was suggested that this patient had a mutation in the *CD20* gene as onset of primary lymphoma. Because normal and mutated *CD20* gene were almost the same copy numbers and the most of cells in the lymph follicle were stained in L26 at the first diagnosis, it can be considered that the lymphoma cells of this patient had equal number of normal and mutated *CD20* alleles rather than the mixture of the cells having only normal *CD20* allele(s) or only mutant allele(s). And at the relapse, two cell populations of the different affinity for rituximab has arose ('R-high' and 'R-low'), and both had a genome of the same mutation status, however, the expression of the mutated mRNA has been predominant only in 'R-low'. As a result of semi-quantitative RT-PCR analysis revealed that whole *CD20* mRNA expression of 'R-low' slightly decreased as compared with that of 'R-high' (data not shown), the imbalanced mRNA expression in 'R-low' may be due to the suppression of *CD20* mRNA expression from the wild-type allele at the transcription level.

To summarize these data, the primary lymphoma cells of this patient expressed both wild-type and mutated *CD20* equally. As the mutant CD20 in this case was found to have little effect on the antigenicity of wild-type CD20 molecules, these cells were still susceptible to rituximab plus CHOP and the patient has obtained complete remission. However, at the relapse, cells that predominantly expressed the mutant CD20 emerged. This mutant molecule expressed and localized at the plasma membrane, however, the large loop could not be oriented appropriately. So it was considered that rituximab-containing salvage treatments have failed perhaps because affinity for rituximab was not enough.

It was noteworthy that the antibody that recognizes N-terminal region of CD20 has capability to detect the mutated CD20 before start of the salvage therapy. This indicated the possibility that we can predict the existence of lymphoma cells resistant to rituximab before start of therapy. In addition, this information may provide important criterion to judge whether it should switch to the treatment such as using second-generation CD20 antibody that is effective against fewer CD20-expressing cells[9–12] or using antibody for the different target molecule such as CD22.[13,14]

The resistance for a molecular target drug acquired by a mutation in the gene of the target molecule is commonly considered to be irreversible.[15–19] We propose here that detecting a mutation in the gene by screening using antibodies of two kinds of epitope is useful in detection of irreversible resistant mutation for molecular targeted drug including rituximab.

Conflict of interest

The authors declare no conflict of interest.

Acknowledgements

We thank Ms Sayuri Minowa, Ms Harumi Shibata and Ms Mariko Mikuniya for their assistance in specimen preparation. We also thank Dr Dovie Wylie of On-Site English, Inc. (Palo Alto, CA, USA) for English editing assistance.

References

1 Terui Y, Mishima Y, Sugimura N, Kojima K, Sakurai T, Kuniyoshi R *et al.* Identification of CD20 C-terminal deletion mutations associated with loss of CD20 expression in non-Hodgkin's lymphoma. *Clin Cancer Res* 2009; **15**: 2523–2530.
2 Mason DY, Comans-Bitter WM, Cordell JL, Verhoeven MA, van Dongen JJ. Antibody L26 recognizes an intracellular epitope on the B-cell-associated CD20 antigen. *Am J Pathol* 1990; **136**: 1215–1222.
3 Norton AJ, Isaacson PG. Monoclonal antibody L26: an antibody that is reactive with normal and neoplastic B lymphocytes in routinely fixed and paraffin wax embedded tissues. *J Clin Pathol* 1987; **40**: 1405–1412.
4 Hata H, Matsuzaki H, Matsuno F, Sonoki T, Takemoto S, Kuribayashi N *et al.* Establishment of a monoclonal antibody to plasma cells: a comparison with CD38 and PCA-1. *Clin Exp Immunol* 1994; **96**: 370–375.
5 Kohler G, Milstein C. Continuous cultures of fused cells secreting antibody of predefined specificity. *Nature* 1975; **256**: 495–497.
6 Mishima Y, Sugimura N, Matsumoto-Mishima Y, Terui Y, Takeuchi K, Asai S *et al.* An imaging-based rapid evaluation method for complement-dependent cytotoxicity discriminated clinical response to rituximab-containing chemotherapy. *Clin Cancer Res* 2009; **15**: 3624–3632.
7 Polyak MJ, Li H, Shariat N, Deans JP. CD20 homo-oligomers physically associate with the B cell antigen receptor. Dissociation upon receptor engagement and recruitment of phosphoproteins and calmodulin-binding proteins. *J Biol Chem* 2008; **283**: 18545–18552.
8 Johnson NA, Leach S, Woolcock B, deLeeuw RJ, Bashashati A, Sehn LH *et al.* CD20 mutations involving the rituximab epitope are rare in diffuse large B-cell lymphomas and are not a significant cause of R-CHOP failure. *Haematologica* 2009; **94**: 423–427.
9 Pawluczkowycz AW, Beurskens FJ, Beum PV, Lindorfer MA, van de Winkel JG, Parren PW *et al.* Binding of submaximal C1q promotes complement-dependent cytotoxicity (CDC) of B cells opsonized with anti-CD20 mAbs ofatumumab (OFA) or rituximab (RTX): considerably higher levels of CDC are induced by OFA than by RTX. *J Immunol* 2009; **183**: 749–758.
10 Hagenbeek A, Gadeberg O, Johnson P, Pedersen LM, Walewski J, Hellmann A *et al.* First clinical use of ofatumumab, a novel fully human anti-CD20 monoclonal antibody in relapsed or refractory follicular lymphoma: results of a phase 1/2 trial. *Blood* 2008; **111**: 5486–5495.
11 Patz M, Isaeva P, Forcob N, Muller B, Frenzel LP, Wendtner CM *et al.* Comparison of the *in vitro* effects of the anti-CD20 antibodies rituximab and GA101 on chronic lymphocytic leukaemia cells. *Br J Haematol* 2011; **152**: 295–306.
12 Mossner E, Brunker P, Moser S, Puntener U, Schmidt C, Herter S *et al.* Increasing the efficacy of CD20 antibody therapy through the engineering of a new type II anti-CD20 antibody with enhanced direct and immune effector cell-mediated B-cell cytotoxicity. *Blood* 2010; **115**: 4393–4402.
13 Dijoseph JF, Dougher MM, Armellino DC, Evans DY, Damle NK. Therapeutic potential of CD22-specific antibody-targeted chemotherapy using inotuzumab ozogamicin (CMC-544) for the treatment of acute lymphoblastic leukemia. *Leukemia* 2007; **21**: 2240–2245.
14 DiJoseph JF, Goad ME, Dougher MM, Boghaert ER, Kunz A, Hamann PR *et al.* Potent and specific antitumor efficacy of CMC-544, a CD22-targeted immunoconjugate of calicheamicin, against systemically disseminated B-cell lymphoma. *Clin Cancer Res* 2004; **10**: 8620–8629.
15 Pao W, Miller VA, Politi KA, Riely GJ, Somwar R, Zakowski MF *et al.* Acquired resistance of lung adenocarcinomas to gefitinib or

erlotinib is associated with a second mutation in the EGFR kinase domain. *PLoS Med* 2005; **2**: e73.
16 Engelman JA, Janne PA. Mechanisms of acquired resistance to epidermal growth factor receptor tyrosine kinase inhibitors in non-small cell lung cancer. *Clin Cancer Res* 2008; **14**: 2895–2899.
17 Shah NP, Sawyers CL. Mechanisms of resistance to STI571 in Philadelphia chromosome-associated leukemias. *Oncogene* 2003; **22**: 7389–7395.
18 Shah NP, Nicoll JM, Nagar B, Gorre ME, Paquette RL, Kuriyan J *et al.* Multiple BCR-ABL kinase domain mutations confer polyclonal resistance to the tyrosine kinase inhibitor imatinib (STI571) in chronic phase and blast crisis chronic myeloid leukemia. *Cancer Cell* 2002; **2**: 117–125.
19 Wang SE, Narasanna A, Perez-Torres M, Xiang B, Wu FY, Yang S *et al.* HER2 kinase domain mutation results in constitutive phosphorylation and activation of HER2 and EGFR and resistance to EGFR tyrosine kinase inhibitors. *Cancer Cell* 2006; **10**: 25–38.

The Impact of Superior Mediastinal Lymph Node Metastases on Prognosis in Non-small Cell Lung Cancer Located in the Right Middle Lobe

Yukinori Sakao, MD, PhD, Sakae Okumura, MD,* Mun Mingyon, MD, PhD,* Hirofumi Uehara, MD, PhD,* Yuichi Ishikawa, MD, PhD,† and Ken Nakagawa, MD**

Background: We aimed to assess hilar and mediastinal lymph node involvement and its impact on prognosis in patients with right middle lobe lung cancer.

Methods: The records of 170 patients undergoing surgery for right middle lobe non-small cell lung cancer from 1980 to December 2007 were retrospectively examined. There were 45 patients found to have hilar or mediastinal lymph nodes metastases. This subgroup included 31 N2 patients and 14 N1 patients, and included 23 women and 22 men, whose ages ranged from 32 to 83 years (median = 61 years). The status of mediastinal, hilar, and interlobar lymph nodes was assessed according to the seventh edition of the TNM classification for lung cancer. Patient records were examined for age, gender, preoperative nodal status, surgical procedure, metastatic status of lymph nodes (distribution and numbers), tumor size, and histologic features (cell type and differentiation degree). Survival duration was defined as the interval between surgery and death from the tumor or the most recent follow-up.

Results: For N1 cases (n = 14), the most frequent metastatic site was #12m (lymph nodes adjacent to the middle lobe bronchus), which occurred in 11 cases; there was one case with metastases in #11s (lymph nodes between the upper lobe bronchus and bronchus intermedius), and no case with #11i metastases (lymph nodes between the right middle and lower lobe bronchi). The most frequent metastatic mediastinal zone was the subcarinal zone (25/31), and the superior mediastinal zone also had a high incidence of metastases (22/31). Sixteen cases had metastases to both the superior and subcarinal zones, and six cases had metastasis to superior mediastinal zone without subcarinal zone metastasis. When #11s or #11i was involved, eight of nine or five of five, respectively, were N2 cases. Univariate analyses revealed that tumor diameter, cN, status of lymph node metastases, and operative procedure (pneumonectomy) were significant prognostic factors in N2 cases. Regarding status of lymph node metastases, superior mediastinal zone metastases, both superior and inferior (subcarinal) zone metastases, and #11i were significant prognostic factors. Because #11i metastases and superior mediastinal lymph nodes metastases were highly correlated with each other (p = 0.02), two separate models were used in multivariate analyses. Superior mediastinal metastases (p = 0.03) and #11i metastases (p = 0.015) were revealed to be significant independent prognostic factors, whereas multiple-zone metastases only tended toward significance as an adverse prognostic factor (p = 0.054).

Conclusions: Superior mediastinal lymph node metastases and #11i metastases were significant adverse prognostic factors in patients with middle lobe lung cancer, and they were associated with each other.

Key Words: Middle lobe cancer, Superior mediastinal lymph node metastasis, N2, NSCLC.

(*J Thorac Oncol.* 2011;6: 494–499)

The right middle lobe is the smallest lobe in the lung, and lung cancer originating there is much less common than in the other lobes, occurring in 3.8 to 6.7% of all lung cancers.[1–4] The fact that it is less common may be a reason that there are a few reports on the prognostic factors of middle lobe lung cancer.

Lymph drainage from the middle lobe extends to both superior and inferior mediastinal lymph nodes, and previous reports have demonstrated a high incidence of metastases to both the superior and inferior mediastinal zones.[1–6] Nevertheless, there are few articles on the relationships between status of hilar and mediastinal lymph node metastases and patient prognoses.

In this retrospective study, we aimed to clarify prognostic factors in patients with middle lobe lung cancer who underwent surgery. Furthermore, we wanted to determine the association between the status of lymph node metastases and postoperative prognosis.

PATIENTS AND METHODS

This was a retrospective study. Because individual patients were not identified, our institutional review board waived the requirement for obtaining patient consent and approved this study. Between 1980 and December 2007, 170 patients underwent surgical resection at the Cancer Institute

Departments of *Thoracic Surgical Oncology and †Pathology, Japanese Foundation for Cancer Research, Cancer Institute Hospital, Tokyo, Japan.

Disclosure: The authors declare no conflicts of interest.

Address for correspondence: Yukinori Sakao, MD, PhD, Department of Thoracic Surgical Oncology, Japanese Foundation for Cancer Research, Cancer Institute Hospital, 3-10-6, Ariake, Koto-ku, Tokyo 135-8550, Japan. E-mail: yukinori.sakao@jfcr.or.jp

ISSN: 1556-0864/11/0603-0494

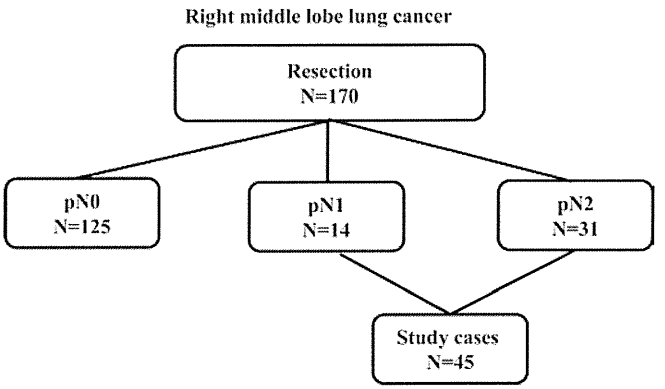

FIGURE 1. Study group subdivisions. Between 1980 and December 2007, 170 patients underwent surgical resections for right middle lobe lung cancer at the Cancer Institute Hospital. There were 14 N1 cases and 31 N2 cases evaluated.

Hospital for primary lung cancer originating in the right middle lobe. Among these patients, 45 were diagnosed with N1 or N2 disease after lung resection and hilar and mediastinal node dissections (Figure 1). The extent of lymph node dissection was not affected by a suspicion of N1 disease. We have routinely performed nearly the same dissection (ND2a).

All the 45 study patients were confirmed for their prognoses. The primary surgical procedure for lymph node dissection, such as hilar and mediastinal nodal dissection, was established in Japan in the late 1970s. In our institute, the extent of lymph node dissection conducted recently is nearly the same as that during the 1980s. Some cases had sampling due to disorders such as cardiac or pulmonary, and these cases were excluded from this study. The resected lymph nodes were separated according to the map[7] in the operating room by the surgeons. Station 10 nodes dissected in middle lobe cancer were adjacent to the inferior parts of the main bronchus, and these nodes were included in the subcarinal zone according to the new TNM. [7] The other station 10 nodes, which were adjacent to the upper parts of the main bronchus, were not routinely dissected, and this area is difficult to dissect without an upper lobectomy.

This subgroup included 31 N2 patients and 14 N1 patients, and included 23 women and 22 men, whose ages ranged from 32 to 83 years (median = 61 years, Table 1). For all patients, preoperative staging was performed using chest computed tomography (CT), abdominal CT or ultrasonography, brain CT or magnetic resonance imaging, and bone scans. Clinical mediastinal and hilar lymph node status was assessed as positive if the chest CT showed that the short axis of a node was more than 1.0 cm. CT scans have been used for evaluating lung cancer staging in our institute since 1980. Of course, CT imaging quality is different when comparing that in the 1980s with that in the 2000s. Nevertheless, this study focused on pathological N status of middle lobe lung cancer, and the quality of pathological examinations was nearly the same during the study period. We excluded those patients who had induction therapy because it seemed to be difficult to evaluate their pathological node status.

TABLE 1. Patient Characteristics

Age (yr)	32–83, median: 61
Gender (male/female)	22/23
c-N	
N0/N1/N2	23/14/8
c-T	
T1/T2/T3/T4	17/24/3/1
p-N	
N1/N2	14/31
Histologic type	
Adenocarcinoma/others	35/10
Well-differentiated/others	10/35
Surgical procedure	
Lobectomy/bilobectomy/pneumonectomy	21/14/10

Bulky N2 (shortest mediastinal lymph node diameter >2 cm) patients have not been candidates for surgery in our institute. Although mediastinoscopy, 18F-fluorodeoxyglucose positron emission tomography, or endobronchial ultrasound with transbronchial needle aspiration was applied to some patients in this series, they were not used for preoperative staging. Follow-up periods ranged from 2 to 302 months (median follow-up for living patients was 86 months).

The status of mediastinal, hilar, or interlobar nodes was assessed according to the seventh edition of the TNM classification for lung cancer.[7] Mediastinal nodes were classified into the following three zones: superior, subcarinal, and inferior. N1 nodes were classified into two zones as hilar or interlobar, and peripheral. The interlobar zone was divided into three subgroups as follows: #12m, lymph nodes adjacent to the middle lobe bronchus; #11s, lymph nodes between the upper lobe bronchus and bronchus intermedius; and #11i, lymph nodes between the right middle and lower lobe bronchi. When a case had mediastinal nodal involvement of two or more zones, it was classified with multiple-zone metastases.

Patient characteristics are summarized in Table 1. Patient records were examined for age, gender, preoperative nodal status, surgical procedure, metastatic status of lymph nodes (distribution and numbers), tumor size, and histologic features (cell type and degree of differentiation).

Statistical Analysis

Survival duration was defined as the interval between surgery and death from the tumor, or the most recent follow-up. Survival rates were calculated using the Kaplan-Meier method. Univariate analyses were performed using the log-rank test, χ^2 test, and logistic regression. Multivariate analyses were performed for variables with p values less than 0.1 by univariate analysis, using the logistic regression test in StatView J 5.0 (SAS Institute Inc., Cary, NC). A p value less than 0.05 was considered significant.

RESULTS

Status of Lymph Node Metastases

In N1 cases (n = 14), the most frequent metastatic site was #12m, occurring in 11 cases, and there was one case with metastases in #11s and 0 cases with #11i metastases (Figure 2).

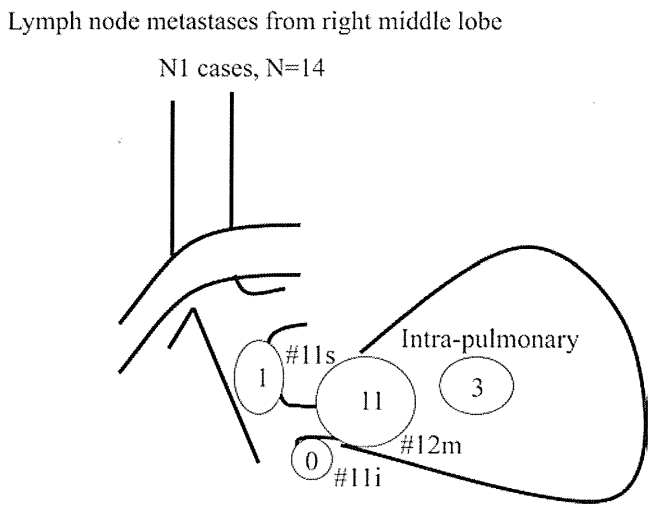

FIGURE 2. Distribution of metastatic nodes in N1 cases.

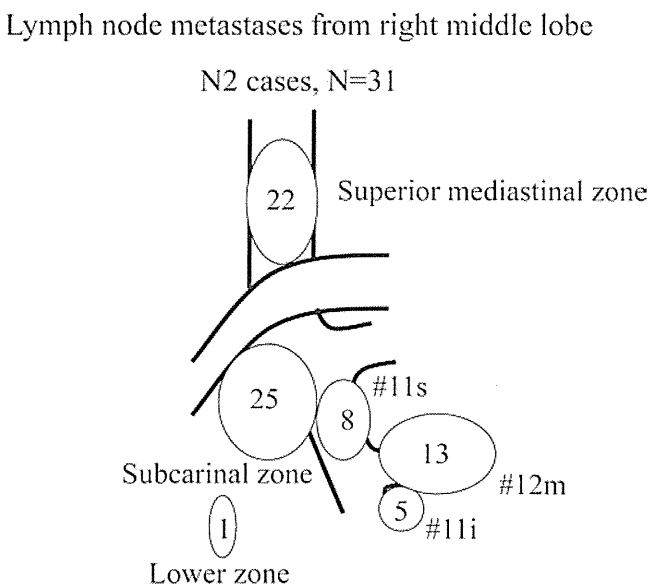

FIGURE 3. Distribution of metastatic nodes in N2 cases.

The most frequent metastatic mediastinal zone was the subcarinal zone (25/31 N2 cases). The superior zone also had a high incidence of metastases (22/31 cases). There were 16 cases with metastases in both the superior and subcarinal zones; nine cases were metastasized to the subcarinal zone without the superior mediastinal zone metastasis, and six cases were metastasized to superior the mediastinal zone without the subcarinal zone metastasis (Figure 3). When #11s was involved, eight of nine cases were N2, and when #11i was involved, all five cases were N2 (Figures 4 and 5).

Survival Rates for Patients with Nodal Involvement

The postoperative 5-year survival rate for patients with N1 was 62% and with N2 was 20% ($p = 0.02$). The postoperative 5-year survival rate was 83% for 125 N0 patients. The prognoses for N0 patients with right middle lobe cancers were not different from those of N0 patients with other involved lobes.

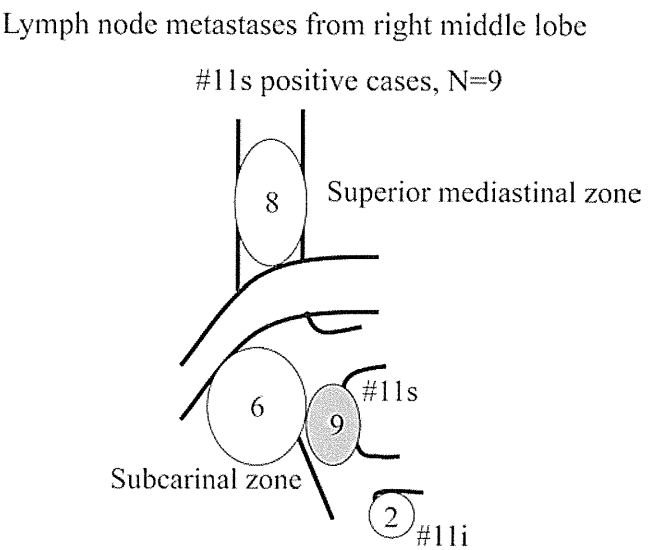

FIGURE 4. Association of #11s metastases with mediastinal zone metastases.

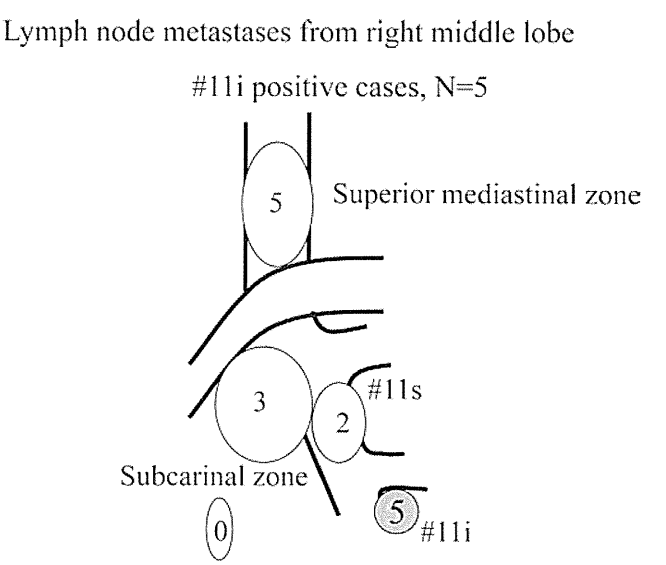

FIGURE 5. Association of #11i metastases with mediastinal zone metastases.

Prognostic Factors for N2 in the Right Middle Lobe

Univariate analyses using the variables listed in Table 2 showed that diameter, cN1–2/cN0, status of lymph node metastases, and operative procedure (pneumonectomy) were significant prognostic factors. Nevertheless, there was no difference in prognoses between lobectomy and bilobectomy. Regarding specific prognostic lymph node metastases, superior mediastinal zone metastases, both superior and subcarinal and interlobar #11i metastases were significant prognostic factors. Inferior mediastinal zone metastases, and #12m and

TABLE 2. Prognostic Factors for Patients with N2: Univariate Analysis

Variables	Cases	5-yr Survival (%)	*p*
Gender			
Male/female	14/17	17.8/22.0	0.95
Age			
<70 yr/70 yr or older	22/9	21.7/16.0	0.37
Diameter (14–65 mm, mean: 35 mm)			
<35 mm/35 mm or larger	16/15	36.5/6.8	0.02
cN			
cN1–2/cN0	15/16	8.0/33.7	0.042
cN0–1/cN2	23/8	23.3/12.5	0.24
Adenocarcinoma/others	26/5	25.2/0	0.1
Well differentiated/others	6/25	16.7/21.5	0.81
Pleural involvement yes/no	15/16	21.8/17.3	0.57
Status of lymph node metastases			
Superior mediastinal zone yes/no	22/9	6.4/50.8	0.005
Inferior mediastinal zone yes/no	25/6	21.4/16.7	0.61
#12m yes/no	13/18	24.7/18.3	0.92
#11s yes/no	8/23	14.3/21.9	0.14
#11i yes/no	5/26	0/23.6	0.02
Both superior and inferior zones			
Multiple zones/single zone	16/15	0/36.4	0.01
Operative procedure			
Pneumonectomy vs. others	7/24	0/25.8	0.009
Lobectomy vs. bilobectomy	16/8	23.6/29.2	0.61
Period			
Before 1995 vs. from and after 1995	15/16	13.3/28.4	0.28

#12m, lymph nodes adjacent to middle lobe bronchus; #11s, lymph nodes between the upper lobe bronchus and bronchus intermedius; #11i, lymph nodes between the right middle and lower lobe bronchi.

TABLE 3. Prognostic Factors for Patients with N2: Multivariate Analysis

Variables	Odds Ratio	95% CI	*p*
Model 1			
Diameter	1.04	0.99–1.08	0.054
cN			
cN1–2/cN0	1.87	0.71–4.95	0.21
Status of lymph node metastases			
Superior mediastinal zone	5.08	1.20–21.8	0.03
Multiple zones	1.42	0.51–3.96	0.50
Operative procedure			
Pneumonectomy	1.13	0.30–4.34	0.88
Model 2			
Diameter	1.03	0.99–1.06	0.17
cN			
cN1–2/cN0	1.38	0.54–3.52	0.51
Status of lymph node metastases			
#11i	4.80	1.34–17.0	0.015
Multiple zones	2.80	0.98–7.96	0.054
Operative procedure			
Pneumonectomy	2.32	0.62–10.0	0.20

#11i, lymph nodes between the right middle and lower lobe bronchi.

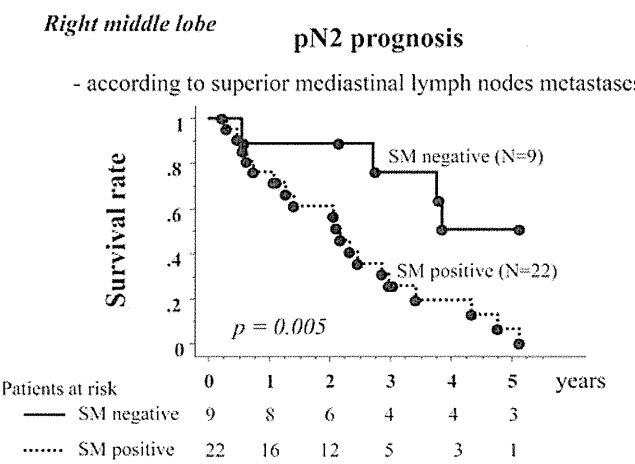

FIGURE 6. Postoperative survival according to superior mediastinal nodal involvement.

#11s metastases were not significant. There was no difference in prognoses between the patients before 1995 and patients from 1996 and after (5-year survivals of 13.3% and 28.4%; $p = 0.28$).

Significant variables by univariate analyses were analyzed by multivariate analyses (Table 3, models 1 and 2). Because #11i metastases and superior mediastinal lymph nodes metastases were highly correlated with each other ($p = 0.02$), two separate models were used for multivariate analyses. In model 1, superior mediastinal metastases were revealed to be a significant independent prognostic factor ($p = 0.03$). In model 2, #11i metastases were revealed to be a significant independent prognostic factor ($p = 0.015$), whereas multiple zone metastases only tended toward significance as an adverse prognostic factor ($p = 0.054$).

Survival Rate According to Prognostic N2 Factors

N2 patients were categorized according to whether they had significant prognostic factors determined from multivariate analyses, including superior mediastinal lymph nodes metastases, #11i metastases, or multiple mediastinal metastatic zones.

The 5-year survival rate was 50.8% in patients without superior mediastinal lymph nodes metastases, whereas it was 6.4% in patients with superior mediastinal lymph node metastases ($p = 0.005$, Figure 6). The 5-year survival rate was 23.6% in patients without #11i lymph node metastases, whereas there were no long-term survivors (dead within 3 years) in patients with #11i lymph node metastases ($p = 0.008$, Figure 7). Furthermore, the 3-year and 5-year survival rates were 58.2% and 36.4% in patients with single-zone mediastinal lymph node metastases, whereas they were 29.6% and 0% in patients with multiple-zone mediastinal lymph node metastases ($p = 0.01$), respectively. Nevertheless, by multivariate analysis, superior mediastinal lymph

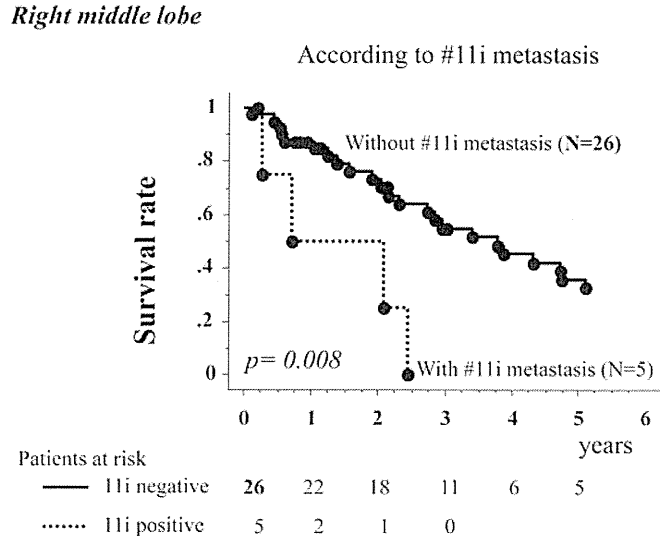

FIGURE 7. Postoperative survival according to #11i nodal involvement.

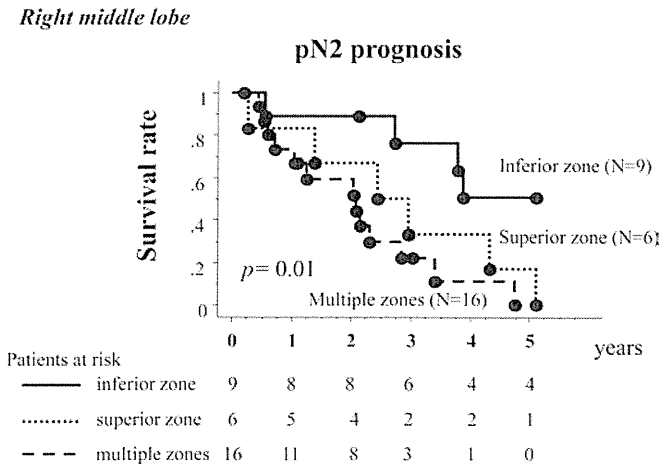

FIGURE 8. Postoperative survival: comparison of superior mediastinal nodal involvement with multiple-zone metastases.

node metastases were revealed to be a stronger prognostic factor than multiple metastatic zones (Figure 8).

DISCUSSION

There have been many reports on the prognostic impact of metastasis to specific mediastinal zones, especially lung cancer in the upper or lower lobes. For patients with lung cancer with tumor originating in the upper lobe or division, the frequency of subcarinal lymph node metastases has been reported to range from 3 to 5%, with the 5-year survival rates ranging from 9 to 18%.[8–10] The frequency of superior mediastinal lymph node metastases has been reported to range from 4 to 5%, with 5-year survival rates ranging from 0 to 19%.[10,11] This low-frequency mediastinal lymph node involvement was highly associated with multilevel N2, and therefore, the outcomes were poor.[10,12,13] In this study, the frequency of metastases was similar for the subcarinal and superior mediastinal zones, and the incidences in N2 patients were 80.6% and 71.0%, respectively. Thus, both superior and inferior mediastinal zones were found to be major metastatic sites, and these results are compatible with previous reports.[14]

We have revealed that metastases to the superior mediastinal lymph nodes are an important independent prognostic factor in patients with N2 middle lobe cancer. This is similar to what is seen in lower lobe cancer. Nevertheless, the incidence of skip metastasis to the superior mediastinum is very different between cancer in the middle lobe and in the lower lobe. The incidence in this study was 20% for N2 and has been reported to range from 3 to 4.5% in N2 right lower lobe cancer.[10–12] Furthermore, there was a significant difference in the 5-year survival rates for superior mediastinal involvement and inferior mediastinal involvement (6.5% and 50.8%, respectively), even for single-zone N2. When superior mediastinal lymph nodes were involved, the prognosis was almost the same as for multilevel N2 patients with middle lobe cancer.

The most frequent metastatic hilar lymph node was #12m, and most #11s and #11i metastases were found in N2 patients. In other words, metastases found in #11s or #11i indicate N2 disease (#11s: 8/9 and #11i: 5/5). Surprisingly, interlobar (lower lobe: #11i) lymph node involvement was an important adverse prognostic factor, even in N2 patients. This may be explained by the fact that there was an association between #11i metastases and superior mediastinal nodal involvement. Metastasis in #11i may be understood to be a result of mediastinal nodal involvement. That is, #11i metastasis is retrograde because of disturbed antegrade lymph drainage to the superior mediastinum from mediastinal metastases. Unfortunately, we could not find any previous reports regarding this correlation between #11i and superior mediastinal node involvement. Further investigation is needed to prove the hypothesis that #11i metastases result from superior mediastinal lymph node metastases.

In conclusion, superior mediastinal lymph node metastases and #11i metastases were significant adverse prognostic factors in patients with middle lobe lung cancer, and they were associated with each other. Furthermore, in patients with middle lobe lung cancer, #11i metastases may result from mediastinal metastases, and the impact on prognosis must be different from that of patients with cancer in other lobes.

Limitations of this study include its retrospective nature, including cases from the 1980s, a small sample number, and that routine adjuvant chemotherapy for N2 patients was started in 2006. Therefore, in this study, it was difficult to evaluate the effects on prognosis with respect to adjuvant chemotherapy.

REFERENCES

1. Vincent RG, Takita H, Lane WW, et al. Surgical therapy of lung cancer. *J Thorac Cardiovasc Surg* 1976;71:581–591.
2. Freise G, Gabler A, Liebig S. Bronchial carcinoma and long-term survival. Retrospective study of 433 patients who underwent resection. *Thorax* 1978;33:228–234.

3. Gifford JH, Waddington JKB. Review of 464 cases of carcinoma of lung treated by resection. *Br Med* 1957;30:723–730.
4. Ochsner A, Ray CJ, Acreea PW. Cancer of lung; review of experiences with 1457 cases of bronchogenic carcinoma. *Am Rev Tuberc* 1954;70:763–783.
5. Riquet M, Dupont P, Hidden G, et al. Lymphatic drainage of the middle lobe of the adult lung. *Surg Radio Anat* 1990;12:231–233.
6. Hata E, Hayakawa K, Miyamoto H, et al. Rationale for extended lymphadenectomy for lung cancer. *Thorac Surg* 1990;5:19–25.
7. Rusch VW, Asamura H, Watanabe H, et al. Members of IASLC Staging Committee. The IASLC lung cancer staging project: a proposal for a new international lymph node map in the forthcoming seventh edition of the TNM classification for lung cancer. *J Thorac Oncol* 2009;4:1043–1045.
8. Asamura H, Nakayama H, Kondo H, et al. Lobe-specific extent of systematic lymph node dissection for non-small cell lung carcinomas according to a retrospective study of metastasis and prognosis. *J Thorac Cardiovasc Surg* 1999;117:1102–1111.
9. Uehara H, Okumura S, Satoh Y, et al. Validity of omission of subcarinal lymph node dissection in patients with cancer of the right upper lobe or left upper division of the lung. *Jpn J Lung Cancer* 2008;48:266–272.
10. Okada M, Sakamoto T, Yuki T, et al. Border between N1 and N2 stations in lung carcinoma: lessons from lymph node metastatic patterns of lower lobe tumors. *J Thorac Cardiovasc Surg* 2008;129: 825–830.
11. Uehara H, Sakao Y, Mun M, et al. Prognostic value and significance of subcarinal and superior mediastinal lymph node metastasis in lower lobe tumours. *Eur J Cardiothorac Surg* 2010;38:498–502.
12. Ichinose Y, Kato H, Koike T, et al. Japanese Clinical Oncology Group. Completely resected stage IIIA non-small cell lung cancer: the significance of primary tumor location and N2 station. *J Thorac Cardiovasc Surg* 2001;122:803–808.
13. Sakao Y, Miyamoto H, Yamazaki A, et al. The prognostic significance of metastasis to the highest mediastinal lymph node in non-small cell lung cancer. *Ann Thorac Surg* 2006;81:292–297.
14. Naruke T, Tsuchiya R, Kondo H, et al. Lymph node sampling in lung cancer: how should it be done? *Eur J Cardiothorac Surg* 1999;16:S17–S24.

International Association for the Study of Lung Cancer/American Thoracic Society/European Respiratory Society International Multidisciplinary Classification of Lung Adenocarcinoma

William D. Travis, MD, Elisabeth Brambilla, MD, Masayuki Noguchi, MD, Andrew G. Nicholson, MD, Kim R. Geisinger, MD, Yasushi Yatabe, MD, David G. Beer, PhD, Charles A. Powell, MD, Gregory J. Riely, MD, Paul E. Van Schil, MD, Kavita Garg, MD, John H. M. Austin, MD, Hisao Asamura, MD, Valerie W. Rusch, MD, Fred R. Hirsch, MD, Giorgio Scagliotti, MD, Tetsuya Mitsudomi, MD, Rudolf M. Huber, MD, Yuichi Ishikawa, MD, James Jett, MD, Montserrat Sanchez-Cespedes, PhD, Jean-Paul Sculier, MD, Takashi Takahashi, MD, Masahiro Tsuboi, MD, Johan Vansteenkiste, MD, Ignacio Wistuba, MD, Pan-Chyr Yang, MD, Denise Aberle, MD, Christian Brambilla, MD, Douglas Flieder, MD, Wilbur Franklin, MD, Adi Gazdar, MD, Michael Gould, MD, MS, Philip Hasleton, MD, Douglas Henderson, MD, Bruce Johnson, MD, David Johnson, MD, Keith Kerr, MD, Keiko Kuriyama, MD, Jin Soo Lee, MD, Vincent A. Miller, MD, Iver Petersen, MD, PhD, Victor Roggli, MD, Rafael Rosell, MD, Nagahiro Saijo, MD, Erik Thunnissen, MD, Ming Tsao, MD, and David Yankelewitz, MD

Introduction: Adenocarcinoma is the most common histologic type of lung cancer. To address advances in oncology, molecular biology, pathology, radiology, and surgery of lung adenocarcinoma, an international multidisciplinary classification was sponsored by the International Association for the Study of Lung Cancer, American Thoracic Society, and European Respiratory Society. This new adenocarcinoma classification is needed to provide uniform terminology and diagnostic criteria, especially for bronchioloalveolar carcinoma (BAC), the overall approach to small nonresection cancer specimens, and for multidisciplinary strategic management of tissue for molecular and immunohistochemical studies.

Methods: An international core panel of experts representing all three societies was formed with oncologists/pulmonologists, pathologists, radiologists, molecular biologists, and thoracic surgeons. A systematic review was performed under the guidance of the American Thoracic Society Documents Development and Implementation Committee. The search strategy identified 11,368 citations of which 312 articles met specified eligibility criteria and were retrieved for full text review. A series of meetings were held to discuss the development of the new classification, to develop the recommendations, and to write the current document. Recommendations for key questions were graded by strength and quality of the evidence according to the Grades of Recommendation, Assessment, Development, and Evaluation approach.

Results: The classification addresses both resection specimens, and small biopsies and cytology. The terms BAC and mixed subtype adenocarcinoma are no longer used. For resection specimens, new concepts are introduced such as adenocarcinoma in situ (AIS) and minimally invasive adenocarcinoma (MIA) for small solitary adenocarcinomas with either pure lepidic growth (AIS) or predominant lepidic growth with ≤5 mm invasion (MIA) to define patients who, if they undergo complete resection, will have 100% or near 100% disease-specific survival, respectively. AIS and MIA are usually nonmucinous but rarely may be mucinous. Invasive adenocarcinomas are classified by predominant pattern after using comprehensive histologic subtyping with lepidic (formerly most mixed subtype tumors with nonmucinous BAC), acinar, papillary, and solid patterns; micropapillary is added as a new histologic subtype. Variants include invasive mucinous adenocarcinoma (formerly mucinous BAC), colloid, fetal, and enteric adenocarcinoma. This classification provides guidance for small biopsies and cytology specimens, as approximately 70% of lung cancers are diagnosed in such samples. Non-small cell lung carcinomas (NSCLCs), in patients with advanced-stage disease, are to be classified into more specific types such as adenocarcinoma or squamous cell carcinoma,

Affiliations are listed in the appendix.

Disclosure: Valerie W. Rusch, MD, is an active member of the IASLC Staging Committee. Georgio Scagliotti, MD, has received honoraria from Sanofi Aventis, Roche, Eli Lilly, and Astrozeneca. David Yankelevitz, MD, is a named inventor on a number of patents and patent applications relating to the evaluation of diseases of the chest, including measurement of nodules. Some of these, which are owned by Cornell Research Foundation (CRF) are non-exclusively licensed to General Electric. As an inventor of these patents, Dr. Yankelevitz is entitled to a share of any compensation which CRF may receive from its commercialization of these patents. The other authors declare no conflicts of interest.

Address for correspondence: William Travis, MD, Department of Pathology, Memorial Sloan Kettering Cancer Center, 1275 York Avenue, New York, NY 10065. E-mail: travisw@mskcc.org

ISSN: 1556-0864/11/0602-0244

whenever possible for several reasons: (1) adenocarcinoma or NSCLC not otherwise specified should be tested for epidermal growth factor receptor (*EGFR*) mutations as the presence of these mutations is predictive of responsiveness to EGFR tyrosine kinase inhibitors, (2) adenocarcinoma histology is a strong predictor for improved outcome with pemetrexed therapy compared with squamous cell carcinoma, and (3) potential life-threatening hemorrhage may occur in patients with squamous cell carcinoma who receive bevacizumab. If the tumor cannot be classified based on light microscopy alone, special studies such as immunohistochemistry and/or mucin stains should be applied to classify the tumor further. Use of the term NSCLC not otherwise specified should be minimized.

Conclusions: This new classification strategy is based on a multidisciplinary approach to diagnosis of lung adenocarcinoma that incorporates clinical, molecular, radiologic, and surgical issues, but it is primarily based on histology. This classification is intended to support clinical practice, and research investigation and clinical trials. As *EGFR* mutation is a validated predictive marker for response and progression-free survival with EGFR tyrosine kinase inhibitors in advanced lung adenocarcinoma, we recommend that patients with advanced adenocarcinomas be tested for *EGFR* mutation. This has implications for strategic management of tissue, particularly for small biopsies and cytology samples, to maximize high-quality tissue available for molecular studies. Potential impact for tumor, node, and metastasis staging include adjustment of the size T factor according to only the invasive component (1) pathologically in invasive tumors with lepidic areas or (2) radiologically by measuring the solid component of part-solid nodules.

Key Words: Lung, Adenocarcinoma, Classification, Histologic, Pathology, Oncology, Pulmonary, Radiology, Computed tomography, Molecular, *EGFR*, *KRAS*, *EML4-ALK*, Gene profiling, Gene amplification, Surgery, Limited resection, Bronchioloalveolar carcinoma, Lepidic, Acinar, Papillary, Micropapillary, Solid, Adenocarcinoma in situ, Minimally invasive adenocarcinoma, Colloid, Mucinous cystadenocarcinoma, Enteric, Fetal, Signet ring, Clear cell, Frozen section, TTF-1, p63.

(*J Thorac Oncol.* 2011;6: 244–285)

RATIONALE FOR A CHANGE IN THE APPROACH TO CLASSIFICATION OF LUNG ADENOCARCINOMA

Lung cancer is the most frequent cause of major cancer incidence and mortality worldwide.[1,2] Adenocarcinoma is the most common histologic subtype of lung cancer in most countries, accounting for almost half of all lung cancers.[3] A widely divergent clinical, radiologic, molecular, and pathologic spectrum exists within lung adenocarcinoma. As a result, confusion exists, and studies are difficult to compare. Despite remarkable advances in understanding of this tumor in the past decade, there remains a need for universally accepted criteria for adenocarcinoma subtypes, in particular tumors formerly classified as bronchioloalveolar carcinoma (BAC).[4,5] As enormous resources are being spent on trials involving molecular and therapeutic aspects of adenocarcinoma of the lung, the development of standardized criteria is of great importance and should help advance the field, increasing the impact of research, and improving patient care. This classification is needed to assist in determining patient therapy and predicting outcome.

NEED FOR A MULTIDISCIPLINARY APPROACH TO DIAGNOSIS OF LUNG ADENOCARCINOMA

One of the major outcomes of this project is the recognition that the diagnosis of lung adenocarcinoma requires a multidisciplinary approach. The classifications of lung cancer published by the World Health Organization (WHO) in 1967, 1981, and 1999 were written primarily by pathologists for pathologists.[5–7] Only in the 2004 revision, relevant genetics and clinical information were introduced.[4] Nevertheless, because of remarkable advances over the last 6 years in our understanding of lung adenocarcinoma, particularly in area of medical oncology, molecular biology, and radiology, there is a pressing need for a revised classification, based not on pathology alone, but rather on an integrated multidisciplinary platform. In particular, there are two major areas of interaction between specialties that are driving the need for our multidisciplinary approach to classification of lung adenocarcinoma: (1) in patients with advanced non-small cell lung cancer, recent progress in molecular biology and oncology has led to (a) discovery of epidermal growth factor receptor (*EGFR*) mutation and its prediction of response to EGFR tyrosine kinase inhibitors (TKIs) in adenocarcinoma patients[8–11] and (b) the requirement to exclude a diagnosis of squamous cell carcinoma to determine eligibility patients for treatment with pemetrexed, (because of improved efficacy)[12–15] or bevacizumab (because of toxicity)[16,17] and (2) the emergence of radiologic-pathologic correlations between ground-glass versus solid or mixed opacities seen by computed tomography (CT) and BAC versus invasive growth by pathology have opened new opportunities for imaging studies to be used by radiologists, pulmonologists, and surgeons for predicting the histologic subtype of adenocarcinomas,[18–21] patient prognosis,[18–23] and improve preoperative assessment for choice of timing and type of surgical intervention.[18–26]

Although histologic criteria remain the foundation of this new classification, this document has been developed by pathologists in collaboration with clinical, radiology, molecular, and surgical colleagues. This effort has led to the development of terminology and criteria that not only define pathologic entities but also communicate critical information that is relevant to patient management (Tables 1 and 2). The classification also provides recommendations on strategic handling of specimens to optimize the amount of information to be gleaned. The goal is not only longer to solely provide the most accurate diagnosis but also to manage the tissue in a way that immunohistochemical and/or molecular studies can be performed to obtain predictive and prognostic data that will lead to improvement in patient outcomes.

For the first time, this classification addresses an approach to small biopsies and cytology in lung cancer diagnosis (Table 2). Recent data regarding *EGFR* mutation predicting responsiveness to EGFR-TKIs,[8–11] toxicities,[16] and therapeutic efficacy[12–15] have established the importance of distinguishing squamous cell carcinoma from adenocarcinoma and non-small cell lung carcinoma (NSCLC) not otherwise specified (NOS) in patients with advanced lung cancer. Approximately 70% of lung cancers are diagnosed and

TABLE 1. IASLC/ATS/ERS Classification of Lung Adenocarcinoma in Resection Specimens

Preinvasive lesions
Atypical adenomatous hyperplasia
Adenocarcinoma in situ (≤3 cm formerly BAC)
Nonmucinous
Mucinous
Mixed mucinous/nonmucinous
Minimally invasive adenocarcinoma (≤3 cm lepidic predominant tumor with ≤5 mm invasion)
Nonmucinous
Mucinous
Mixed mucinous/nonmucinous
Invasive adenocarcinoma
Lepidic predominant (formerly nonmucinous BAC pattern, with >5 mm invasion)
Acinar predominant
Papillary predominant
Micropapillary predominant
Solid predominant with mucin production
Variants of invasive adenocarcinoma
Invasive mucinous adenocarcinoma (formerly mucinous BAC)
Colloid
Fetal (low and high grade)
Enteric

BAC, bronchioloalveolar carcinoma; IASLC, International Association for the Study of Lung Cancer; ATS, American Thoracic Society; ERS, European Respiratory Society.

staged by small biopsies or cytology rather than surgical resection specimens, with increasing use of transbronchial needle aspiration (TBNA), endobronchial ultrasound-guided TBNA and esophageal ultrasound-guided needle aspiration.[27] Within the NSCLC group, most pathologists can identify well- or moderately differentiated squamous cell carcinomas or adenocarcinomas, but specific diagnoses are more difficult with poorly differentiated tumors. Nevertheless, in small biopsies and/or cytology specimens, 10 to 30% of specimens continue to be diagnosed as NSCLC-NOS.[13,28,29]

Proposed terminology to be used in small biopsies is summarized in Table 2. Pathologists need to minimize the use of the term NSCLC or NSCLC-NOS on small samples and aspiration and exfoliative cytology, providing as specific a histologic classification as possible to facilitate the treatment approach of medical oncologists.[30]

Unlike previous WHO classifications where the primary diagnostic criteria for as many tumor types as possible were based on hematoxylin and eosin (H&E) examination, this classification emphasizes the use and integration of immunohistochemical (i.e., thyroid transcription factor [TTF-1]/p63 staining), histochemical (i.e., mucin staining), and molecular studies, as specific therapies are driven histologic subtyping. Although these techniques should be used whenever possible, it is recognized that this may not always be possible, and thus, a simpler approach is also provided when only H&E-stained slides are available, so this classification may be applicable even in a low resource setting.

METHODOLOGY

Objectives

This international multidisciplinary classification has been produced as a collaborative effort by the International Association for the Study of Lung Cancer (IASLC), the American Thoracic Society (ATS), and the European Respiratory Society. The purpose is to provide an integrated clinical, radiologic, molecular, and pathologic approach to classification of the various types of lung adenocarcinoma that will help to define categories that have distinct clinical, radiologic, molecular, and pathologic characteristics. The goal is to identify prognostic and predictive factors and therapeutic targets.

Participants

Panel members included thoracic medical oncologists, pulmonologists, radiologists, molecular biologists, thoracic surgeons, and pathologists. The supporting associations nominated panel members. The cochairs were selected by the IASLC. Panel members were selected because of special interest and expertise in lung adenocarcinoma and to provide an international and multidisciplinary representation. The panel consisted of a core group (author list) and a reviewer group (Appendix 1, see **Supplemental Digital Content 1** available at http://links.lww.com/JTO/A59, affiliations for coauthors are listed in appendix).

Evidence

The panel performed a systematic review with guidance by members of the ATS Documents Development and Implementation Committee. Key questions for this project were generated by each specialty group, and a search strategy was developed (Appendix 2, see **Supplemental Digital Content 2** available at http://links.lww.com/JTO/A60). Searches were performed in June 2008 with an update in June 2009 resulting in 11,368 citations. These were reviewed to exclude articles that did not have any relevance to the topic of lung adenocarcinoma classification. The remaining articles were evaluated by two observers who rated them by a predetermined set of eligibility criteria using an electronic web-based survey program (www.surveymonkey.com) to collect responses.[31] This process narrowed the total number of articles to 312 that were reviewed in detail for a total of 141 specific features, including 17 study characteristics, 35 clinical, 48 pathologic, 16 radiologic, 16 molecular, and nine surgical (Appendix 2). These 141 features were summarized in an electronic database that was distributed to members of the core panel, including the writing committee. Articles chosen for specific data summaries were reviewed, and based on analysis of tables from this systematic review, recommendations were made according to the Grades of Recommendation, Assessment, Development, and Evaluation (GRADE).[32–37] Throughout the rest of the document, the term GRADE (spelled in capital letters) must be distinguished from histologic grade, which is a measure of pathologic tumor differentiation. The GRADE system has two major components: (1) grading the strength of the recommendation and (2) evaluating the quality of the evidence.[32] The strength of recommendations is based on weighing estimates of benefits versus downsides. Evidence was rated as high, moderate, or low or very low.[32] The

TABLE 2. Proposed IASLC/ATS/ERS Classification for Small Biopsies/Cytology

2004 WHO Classification	SMALL BIOPSY/CYTOLOGY: IASLC/ATS/ERS
ADENOCARCINOMA Mixed subtype Acinar Papillary Solid	*Morphologic adenocarcinoma patterns clearly present:* Adenocarcinoma, describe identifiable patterns present (including micropapillary pattern not included in 2004 WHO classification) Comment: If pure lepidic growth – mention an invasive component cannot be excluded in this small specimen
Bronchioloalveolar carcinoma (nonmucinous)	Adenocarcinoma with lepidic pattern (if pure, add note: an invasive component cannot be excluded)
Bronchioloalveolar carcinoma (mucinous)	Mucinous adenocarcinoma (describe patterns present)
Fetal	Adenocarcinoma with fetal pattern
Mucinous (colloid)	Adenocarcinoma with colloid pattern
Signet ring	Adenocarcinoma with (describe patterns present) and signet ring features
Clear cell	Adenocarcinoma with (describe patterns present) and clear cell features
No 2004 WHO counterpart – most will be solid adenocarcinomas	*Morphologic adenocarcinoma patterns not present (supported by special stains):* Non-small cell carcinoma, favor adenocarcinoma
SQUAMOUS CELL CARCINOMA Papillary Clear cell Small cell Basaloid	*Morphologic squamous cell patterns clearly present:* Squamous cell carcinoma
No 2004 WHO counterpart	*Morphologic squamous cell patterns not present (supported by stains):* Non-small cell carcinoma, favor squamous cell carcinoma
SMALL CELL CARCINOMA	Small cell carcinoma
LARGE CELL CARCINOMA	Non-small cell carcinoma, not otherwise specified (NOS)
Large cell neuroendocrine carcinoma (LCNEC)	Non-small cell carcinoma with neuroendocrine (NE) morphology (positive NE markers), possible LCNEC
Large cell carcinoma with NE morphology (LCNEM)	Non-small cell carcinoma with NE morphology (negative NE markers) – see comment Comment: This is a non-small cell carcinoma where LCNEC is suspected, but stains failed to demonstrate NE differentiation.
ADENOSQUAMOUS CARCINOMA	*Morphologic squamous cell and adenocarcinoma patterns present:* Non-small cell carcinoma, with squamous cell and adenocarcinoma patterns Comment: this could represent adenosquamous carcinoma.
No counterpart in 2004 WHO classification	*Morphologic squamous cell or adenocarcinoma patterns not present but immunostains favor separate glandular and adenocarcinoma components* Non-small cell carcinoma, NOS, (specify the results of the immunohistochemical stains and the interpretation) Comment: this could represent adenosquamous carcinoma.
Sarcomatoid carcinoma	Poorly differentiated NSCLC with spindle and/or giant cell carcinoma (mention if adenocarcinoma or squamous carcinoma are present)

IASLC, International Association for the Study of Lung Cancer; ATS, American Thoracic Society; ERS, European Respiratory Society; WHO, World Health Organization; NSCLC, non-small cell lung cancer; IHC, immunohistochemistry; TTF, thyroid transcription factor.

quality of the evidence expresses the confidence in an estimate of effect or an association and whether it is adequate to support a recommendation. After review of all articles, a writing committee met to develop the recommendations with each specialty group proposing the recommendations, votes for or against the recommendation, and modifications were conducted after multidisciplinary discussion. If randomized trials were available, we started by assuming high quality but down-graded the quality when there were serious methodological limitations, indirectness in population, inconsistency in results, imprecision in estimates, or a strong suspicion of publication bias. If well-done observational studies were available, low-quality evidence was assumed, but the quality was upgraded when there was a large treatment effect or a large association, all plausible residual confounders would diminish the effects, or if there was a dose-response gradient.[36] We developed considerations for good practice related to interventions that usually represent necessary and standard procedures of health care system—such as history taking and physical examination helping patients to make informed decisions, obtaining written consent, or the importance of good communication—when we considered them helpful. In that case, we did not perform a grading of the quality of evidence or strength of the recommendations.[38]

Meetings

Between March 2008 and December 2009, a series of meetings were held, mostly at Memorial Sloan Kettering Cancer Center, in New York, NY, to discuss issues related to

lung adenocarcinoma classification and to formulate this document. The core group established a uniform and consistent approach to the proposed types of lung adenocarcinoma.

Validation

Separate projects were initiated by individuals involved with this classification effort in an attempt to develop data to test the proposed system. These included projects on small biopsies,[39,40] histologic grading,[41–43] stage I adenocarcinomas,[44] small adenocarcinomas from Japan, international multiple pathologist project on reproducibility of recognizing major histologic patterns of lung adenocarcinoma,[45] molecular-histologic correlations, and radiologic-pathologic correlation focused on adenocarcinoma in situ (AIS), and minimally invasive adenocarcinoma (MIA).

The new proposals in this classification are based on the best available evidence at the time of writing this document. Nevertheless, because of the lack of universal diagnostic criteria in the literature, there is a need for future validation studies based on these standardized pathologic criteria with clinical, molecular, radiologic, and surgical correlations.

PATHOLOGIC CLASSIFICATION

Histopathology is the backbone of this classification, but lung cancer diagnosis is a multidisciplinary process requiring correlation with clinical, radiologic, molecular, and surgical information. Because of the multidisciplinary approach in developing this classification, we are recommending significant changes that should improve the diagnosis and classification of lung adenocarcinoma, resulting in therapeutic benefits.

Even after publication of the 1999 and 2004 WHO classifications,[4,5] the former term BAC continues to be used for a broad spectrum of tumors including (1) solitary small noninvasive peripheral lung tumors with a 100% 5-year survival,[46] (2) invasive adenocarcinomas with minimal invasion that have approximately 100% 5-year survival,[47,48] (3) mixed subtype invasive adenocarcinomas,[49–53] (4) mucinous and nonmucinous subtypes of tumors formerly known as BAC,[50–52,54,55] and (5) widespread advanced disease with a very low survival rate.[4,5] The consequences of confusion from the multiple uses of the former BAC term in the clinical and research arenas have been the subject of many reviews and editorials and are addressed throughout this document.[55–61]

Pathology Recommendation 1

We recommend discontinuing the use of the term "BAC." Strong recommendation, low-quality evidence.

Throughout this article, the term BAC (applicable to multiple places in the new classification, Table 3), will be referred to as "former BAC." We understand this will be a major adjustment and suggest initially that when the new proposed terms are used, it will be accompanied in parentheses by "(formerly BAC)." This transition will impact not only clinical practice and research but also cancer registries future analyses of registry data.

CLASSIFICATION FOR RESECTION SPECIMENS

Multiple studies have shown that patients with small solitary peripheral adenocarcinomas with pure lepidic growth may have 100% 5-year disease-free survival.[46,62–68] In addition, a growing number of articles suggest that patients with lepidic predominant adenocarcinomas (LPAs) with minimal invasion may also have excellent survival.[47,48] Recent work has demonstrated that more than 90% of lung adenocarcinomas fall into the mixed subtype according to the 2004 WHO classification, so it has been proposed to use comprehensive histologic subtyping to make a semiquantitative assessment of the percentages of the various histologic components: acinar, papillary, micropapillary, lepidic, and solid and to classify tumors according to the predominant histologic subtype.[69] This has demonstrated an improved ability to address the complex histologic heterogeneity of lung adenocarcinomas and to improve molecular and prognostic correlations.[69]

The new proposed lung adenocarcinoma classification for resected tumors is summarized in Table 1.

TABLE 3. Categories of New Adenocarcinoma Classification Where Former BAC Concept was Used

1. Adenocarcinoma in situ (AIS), which can be nonmucinous and rarely mucinous
2. Minimally invasive adenocarcinoma (MIA), which can be nonmucinous and rarely mucinous
3. Lepidic predominant adenocarcinoma (nonmucinous)
4. Adenocarcinoma, predominantly invasive with some nonmucinous lepidic component (includes some resected tumors, formerly classified as mixed subtype, and some clinically advanced adenocarcinomas formerly classified as nonmucinous BAC)
5. Invasive mucinous adenocarcinoma (formerly mucinous BAC)

BAC, bronchioloalveolar carcinoma.

Preinvasive Lesions

In the 1999 and 2004 WHO classifications, atypical adenomatous hyperplasia (AAH) was recognized as a preinvasive lesion for lung adenocarcinoma. This is based on multiple studies documenting these lesions as incidental findings in the adjacent lung parenchyma in 5 to 23% of resected lung adenocarcinomas[70–74] and a variety of molecular findings that demonstrate a relationship to lung adenocarcinoma including clonality,[75,76] *KRAS* mutation,[77,78] *KRAS* polymorphism,[79] *EGFR* mutation,[80] p53 expression,[81] loss of heterozygosity,[82] methylation,[83] telomerase overexpression,[84] eukaryotic initiation factor 4E expression,[85] epigenetic alterations in the *Wnt* pathway,[86] and FHIT expression.[87] Depending on the extensiveness of the search, AAH may be multiple in up to 7% of resected lung adenocarcinomas.[71,88]

A major change in this classification is the official recognition of AIS, as a second preinvasive lesion for lung adenocarcinoma in addition to AAH. In the category of preinvasive lesions, AAH is the counterpart to squamous dysplasia and AIS the counterpart to squamous cell carcinoma in situ.

Atypical Adenomatous Hyperplasia

AAH is a localized, small (usually 0.5 cm or less) proliferation of mildly to moderately atypical type II pneumocytes and/or Clara cells lining alveolar walls and sometimes, respiratory bronchioles (Figures 1*A, B*).[4,89,90] Gaps are